

ABSTRACT

The oil and gas industry of today is undergoing rapid digitalization. This implies a massive effort to transform standard work procedures and workflows into more efficient practices and implementations using machine learning and automation. This will enable geoscientists to explore and exploit vast amounts of data quickly and efficiently. To address these current industry challenges, we propose a pilot well log database in HDF5 (Hierarchical Data Format version 5) format that can be continuously extended if new data become available. It also provides versatility for data preparation for further analysis. We show an alternative way to store and use log files in a hierarchical structure that is easy to understand and handle by research institutes, companies, and academia. We also touch upon well log depth matching, a long-standing industry challenge, to synchronize data from different logging passes to a single depth reference. Having a robust automated solution for depth matching is important to facilitate use of all available data in a depth interval for analysis by Machine Learning (ML). We propose an automatic well log depth matching workflow capable of handling multiple log types simultaneously, and its integration with the database. The updated depth matched logs are added to the database with their corresponding metadata giving the geoscientist full control. We implemented two algorithms, classical **cross-correlation** combined with a scaling factor to simulate stretch-squeeze effects, and a constrained dynamic time warping (DTW). Our results indicate that the classical **cross-correlation** outperforms the warping for both robustness and speed when the DTW is constrained to avoid excessive signal distortion and when the number of processed curves increases, respectively. Some limitations of our approach are related to large changes in the log patterns between the runs, as well as the assumption of negligible depth shift between log types within the same run. The **cross-correlation** also allows consistent application of depth matching to the metadata. This prototype workflow is tested using two wells from the Norwegian North Sea. We see potential for extending this automatic database-processing workflow to give geoscientists access to all the data to improve interpretation.

INTRODUCTION

Well log databases of practical use to geoscientists and petrophysicists are often limited to standardized curves for a specific rock measurement such as those described in the Norwegian Petroleum Directorate (NPD's) "Blue Book" (NPD, 2019). The "Blue Book" defines which datatypes are mandatory to report and the formats to use. Even though it establishes some data quality requirements, in some cases is not specific enough. This lack of precise specification for data deliverables makes their use difficult. In many cases, addressing the poor data quality in the original raw data files requires the use of very significant data management resources. This is an example of the negative consequences of a lack of attention to data management for preservation of legacy data within the industry. This situation is not only associated with old wells, but also applies to wells currently being drilled. For instance, it is often common to work with a single spliced final density log curve instead of having access to all density measurements acquired at different times during the drilling of the wellbore. Looking at a more complete dataset can give more insight into changes in formation properties during the drilling of the wellbore (temporal framework). Also, since the final logs have undergone several pre-processing steps, usually carried out by third parties, a lot of information is lost during the process. As a result, the end users will have limited information about the history of these curves, how the borehole conditions evolved before, during and after logging, and the impact of the log acquisition dates.

It is also quite common for log analysts to face misalignments or desynchronization issues when using multiple logs as input to an equation set. Misalignment or desynchronization are common both in logs acquired during different and the same logging runs. These mismatches could persist all the way to the final processed curves.

Until now, this issue has been addressed by a sophisticated and expert derived method, with carefully selected depth shifts exactly as needed but remains a challenge in the industry and prevents the use of all the available data. Any petrophysical software packages offer approaches for depth matching/synchronization. Several options are available for automating the process. Manual interventions are nevertheless required to reduce residual misalignment among log curves. This is mainly because depth matching/synchronization of well log data is a crucial step that must be quality controlled as much as possible to keep track of the log curves

misalignment impact, for both qualitative and quantitative interpretations. This often becomes a time-consuming, and tedious process.

In more specialized petrophysical studies, and particularly when training a neural network for ML use, rock physics and seismic property analysis, depth mismatching can be a main source of error. Moreover, the depth mismatching among logs also has a negative impact in traditional workflows and procedures. It can cause poor log correlations, incoherent interpretation, and analysis. This was explained by Zangwill (1982). He proposed a method that integrates analytical and interactive techniques to achieve accurate depth matching. The optimal solution through his method was to achieve a balance between correlation techniques and human capabilities of the expert analyst maximizing the interaction between them. This means that he proposed a curve matching and shifting program based on computerized correlation techniques supervised by an expert operator. He also emphasized the importance of depth matching and possible causes of errors. Depth matching has been researched since the 1960's when automatic dip computations started. These allow for depth matching using correlation of micro resistivity measurements taken at different points along the borehole to correct the dip values.

At the same time, similar work was developed in the pattern recognition field known as the curve matching or pattern matching problem (Myers 1980, Müller 2007). Kerzner (1984) developed software to perform automatic depth matching across wells considering that different logs in the same well can have the same or different deflection behavior for the same formation. He suggested a cross-correlation coefficient as a measure of similarity between the two log curves. Kerzner's method can be split into two steps. The first involves the computation of the correlation coefficients between two logs, and the second selects optimal displacements with a mathematical optimization model. The optimization model is solved via dynamic programming techniques that find the correct shift considering all possible displacements, choosing the shift which minimizes the curve distortion. Anderson and Gaby (1983) applied Dynamic Time Warping (DTW) as a branch of Dynamic Waveform Matching. DTW is a more general tool to correlate well logs which is not limited to linear correlations. These techniques are very popular when combined with dynamic programming for solving problems related to speech, voice, and pattern recognition, data mining, information retrieval, and signal processing among others (Müller 2007). Even though DTW is designed for time series, it can be used for any

type of data that are arranged as an ordered sequence (time or depth series). For this reason, it has been a very popular technique in a variety of fields, especially for well log correlation. DTW is gaining popularity in seismic processing and the seismic-well tie process, for example. Hale (2013) modified the DTW algorithm to solve a common problem in seismic image comparison. Munoz and Hale (2014) and Herrera and van der Baan (2014), proposed an automatic seismic-well tie procedure based on DTW that gives superior results to the classical approach of synthetic generation with manual matching.

Recent work concerning automation of well-log depth matching is presented by Zimmermann et al. (2018), Liang et al. (2019), and Le et al. (2019). They propose a fully automatic workflow that minimizes human intervention by developing a machine learning pipeline. Their approach was implemented for gamma-ray logs from multiple runs in vertical and low deviation wells. It used a fully connected neural network that self-evolve with cloud-based services, and which provides feed-back based on manual adjustments from expert petrophysicists. Their neural network algorithm is based on a classification problem type. At the same time, they developed a metric via a k-majority-voting strategy based on different independent metrics to evaluate the performance of the depth matching process.

We propose as a first stage to build a prototype well log-structured database format that can store acquired data in more optimized formats. The purpose is to allow easy access to all available data and get full control of the logs and metadata associated with them. Our database format also has structures for storing pre-processing stages before the data are ready for petrophysical analysis and machine learning applications. As a second stage, we design a user application to perform depth matching (**signal alignment/synchronization**) on a chosen log suite in an automatic or semi-automatic way offering both **cross-correlation** and DTW algorithms. Even though the former is limited to linear correlations it has the advantage of allowing full user control of the process, and metadata can be depth matched, e.g. temperature, pressure, mud resistivity, etc. Notice that we also consider as metadata some log curves in addition to the traditional metadata as all the parameters and information stated in the file's headers. DTW in contrast is an optimization-based approach that computes the optimal warping path to match two signals, therefore it needs the selection of tuning parameters, and each pair of curves will have a unique warping path that cannot be applied to the metadata (Herrera and van der Baan, 2014). Additionally, we use three different metrics to quantitatively assess the results of the depth matching. They are

Pearson correlation, Euclidean distance, and proportion of trace energy predicted. The user has the option of displaying a log's profile and **cross plots** as a qualitative assessment throughout visual inspection. **We** implement these two stages in two wells from the Ivar Aasen field in the Norwegian sector of the North Sea. These wells differ considerably in terms of the amount of data, drilling and logging planning. The processing time to generate a database containing all the data ranges between minutes to a couple of hours depending on the well complexity. These results can be substantially improved by applying parallelization processing on a GPU, as well as some chunking and compression techniques for data storage. Similarly, the depth matching results show a considerable improvement and reduction in the Pearson correlation, proportional trace energy, and Euclidean distance, respectively computed by both algorithms. The superiority and versatility of the classical **cross-correlation** over DTW for this application is also emphasized, as well as its lower computational cost.

WELL DATA MANAGEMENT AND FORMATS

The increasing use of automation and machine-learning-based approaches for log quality assessment, analysis, and interpretation requires innovative and modern data structure solutions. A flexible assess via Python programming is helpful to ease data assimilation, extraction, and visualization.

The DLIS (Digital Log Interchange Standard) standard from the American Petroleum Institute is a file format designed to solve problems that could not be handled by previously existing formats when more complex logging tools were introduced. Some of these problems that the DLIS format addresses are the variety of data types, e.g. waveforms and arrays, record lengths from a few bits to a thousand bits, and variations in sampling rates recorded during the measuring of a single logging run (Theys, 1999).

Well log files often have complex binary formats containing a vast amount of information such as log measurements, drilling parameters, tools, description of the mnemonic, acquisition equipment (parts), calibration parameters, equipment parameters, among others. With DLIS it is possible to merge, splice and flip log data, record textual data, include records of indefinite length, encryption data, and it avoids limitations related to complex forms of data. However, in some cases changes in logging parameters (metadata) might be absent from these files because they were not acquired nor omission by the operators. Another important information that is not contained in the DLIS format is the depth cranking/tracking performed to correct depth (Theys, 1999).

Besides the lack of depth cranking there is not quantified depth uncertainty information available after the pertinent corrections have been performed by the logging companies, which adds more challenges to obtain accurate depth measurements and complete database. The main challenge associated with this data format is that even though is a followed standard in most cases, vendors and contractors sometimes redefine the standard according to their needs, changing and adding new structures to it that add an additional degree of complexity to read the files. Despite their complexity when it comes to reading and extracting information from the DLIS files have the advantage of having been written during acquisition. Therefore, all acquisition parameters are also recorded at the same time (Equinor, 2019).

To address the industry's future requirements in data management and big data analytics, we propose a hierarchical restructuring of the data information in DLIS files through converting them into a HDF5 file format. HDF5 is an open-source file format developed for managing, organizing, and storing information with their associated metadata, regardless of size and complexity (The HDF Group, 2016). It is a popular file format in the fields of science and engineering. The flexible nature of HDF5 makes it well suited to research applications. During research there is often a need to experiment with different data structures and data processing algorithms. One big advantage of HDF5 is that it is easy to structure the data storage into a format that simplifies subsequent processing steps. A lot of computational and algorithmic complexity can be reduced by storing data in intermediate processing steps. After the research phase is finished, HDF5 is a very high performing and production file format. HDF5 is widespread and there exist bindings for most popular programming languages, for example, Java, C++, C#, Javascript, Python, and Matlab. HDF5 structures and algorithms developed during research can therefore be easily used in commercial/production settings.

The main structure components of HDF5 files are groups, dataset, and attributes. This is also known as part of the building blocks of the HDF5 file data organization and specification. HDF5 is designed to generate a hierarchical organization of heterogeneous data (datasets) into different levels or folders (groups) with their respective metadata (attributes) (The HDF Group, 2016). Fig. 1 illustrates the concept of the HDF5 format and shows the interaction of the main structure components.

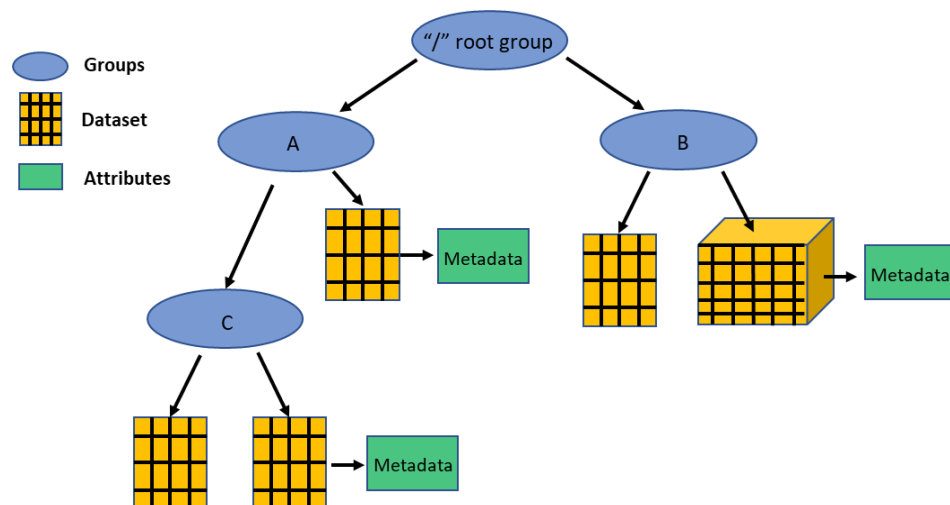


Fig. 1- Example of an HDF5 file structure.

Data restructuring from DLIS to HDF5 file format

We propose a single HDF5 file per well, in other words, an individual HDF5 file containing all data measurements and information from a well. This is simpler than having to deal with multiple DLIS files from a well where each file represents a different logging run.

In Fig. 2 we illustrate how a well log, based on multiple DLIS files, can be organized in a hierarchy. We store the raw data in addition to several stages of processed data in the same HDF5 file. In the illustration the root group represents the well itself. From that we create as many groups as DLIS files exist for a given well. In each group we create subgroups that correspond to the number of depth sampling frames acquired within a logging run. We assign descriptive data or metadata to each frame, followed by the datasets. The datasets are basically the log curves that were acquired during a specific logging run within a frame. Simultaneously, the metadata associated with each log curve is also assigned during this stage. Note that each group level has its own metadata, which is extracted from the DLIS files and storage in the HDF5 file structure. At the hierarchical level of the frames we generate a group called Metadata, which holds several subgroups classifying additional metadata: tools, calibration, coefficients, measurements, equipment, process, and parameters.

We can see the hierarchical buildup of the data as follows. The DLIS files contain a vast amount of data that can be considered as metadata of different datatypes, and it needs to be sorted under the data it belongs to.

For example, the density correction curves should be placed as metadata of the density curve, the monopole acoustic waveforms should be part of the compressional sonic log metadata, and the same occurs for the dipole acoustic waveforms in the case of the shear sonic log, and so on.

As well as the new raw data restructuring, we suggest the inclusion of standardized preprocessing and quality control steps to be followed up. These can be organized in the same manner as subfolders next to the individual runs. They are named as Raw Logs, Depth Shifted Logs, Spliced Logs (optional), and Final Processed Logs.

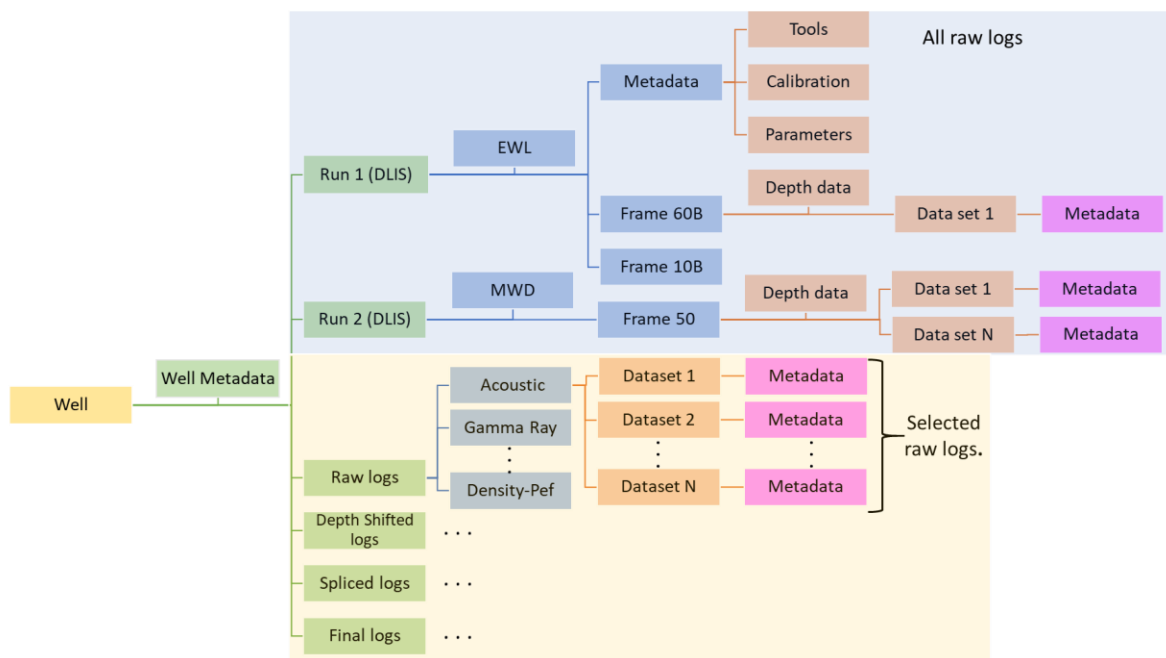


Fig. 2- An example HDF5 file architecture sketch for a single well in which there have been two logging runs. It shows the organization of individual sub-groups associated with each logging run, as well as raw, depth shifted, spliced and final processed log versions within the file structure. The blue square illustrates the structure for the entire data in the file while the yellow square emphasizes the organization and structure of the selected logs categorized by petrophysical properties/measurements (Acoustics, Gamma Ray, Resistivity, Density-Pef, and Neutron) as we move further with process like depth matching and splicing to obtain final logs for petrophysical analysis and interpretation.

The proposed database can be visualized and handled via HDFView application, which is also an open source offered by the HDF5 Group. This is an example of a user interface of our hierarchical log database. Fig. 3 depicts several stages during the database building process visualized with HDFView. First, we create the HDF5 file for a single well generating groups per DLIS file. Later we generate a subgroup for the specific

selection of logs considered for petrophysical analysis classified as Gamma Ray, Resistivity, Density-Pef, etc. **This** stage of selection takes all the logs under specific classification guided by mnemonics, for instance, gamma ray logs named as KBGR, BGRC, ECGR, GR depending on the logging company, which implies that we have a pool of mnemonics per each log measurement. This can be easily expanded by adding new mnemonics to the corresponding list and log category. Afterwards, all the gamma ray logs will be placed under the Gamma Ray folder, and they can be identified through their metadata (Fig. 3a). Additionally, the depth measurement corresponding to each run and therefore to each suite of logs is also placed under the same folder. In the same way, this information is used to perform further selections such as discriminating repeated sections from main logged sections, for example. The database actual manipulation is done via Python coding, we generate several functions that take and transform the selected raw log folders into Python dataframes. Regarding the indexing of the data and to have a better control of the depth measurements two separate dataframes are created one for LWD logs and one for EWL logs per log type. We use the first and the last depth value that has a valid measurement, **in other words, we identify the first and the last value that is different from -999.25 (no data value)** to create a global index vector at the standard depth sampling rate of 0.5 ft (0.1524 m). This allows us to generate individual dataframes per log type, allocating the log sections as concatenated small dataframes in their corresponding depth ranges, one example of this is shown in Fig. 4, where we can see the representation of three sections along the borehole indicated by colors (dataframes) and concatenated into a single big dataframe honoring the corresponding depths based on the global index. Once we create the dataframes along with keywords e.g. log type/log category and mnemonics, those are used as input for a series of sequential functions used to perform the depth matching workflow that we present in this work. **Finally**, the results are retrieved to the database and placed under the Depth Shifted log folder (see Fig. 3b). The same dynamic is thought for the subsequent steps.

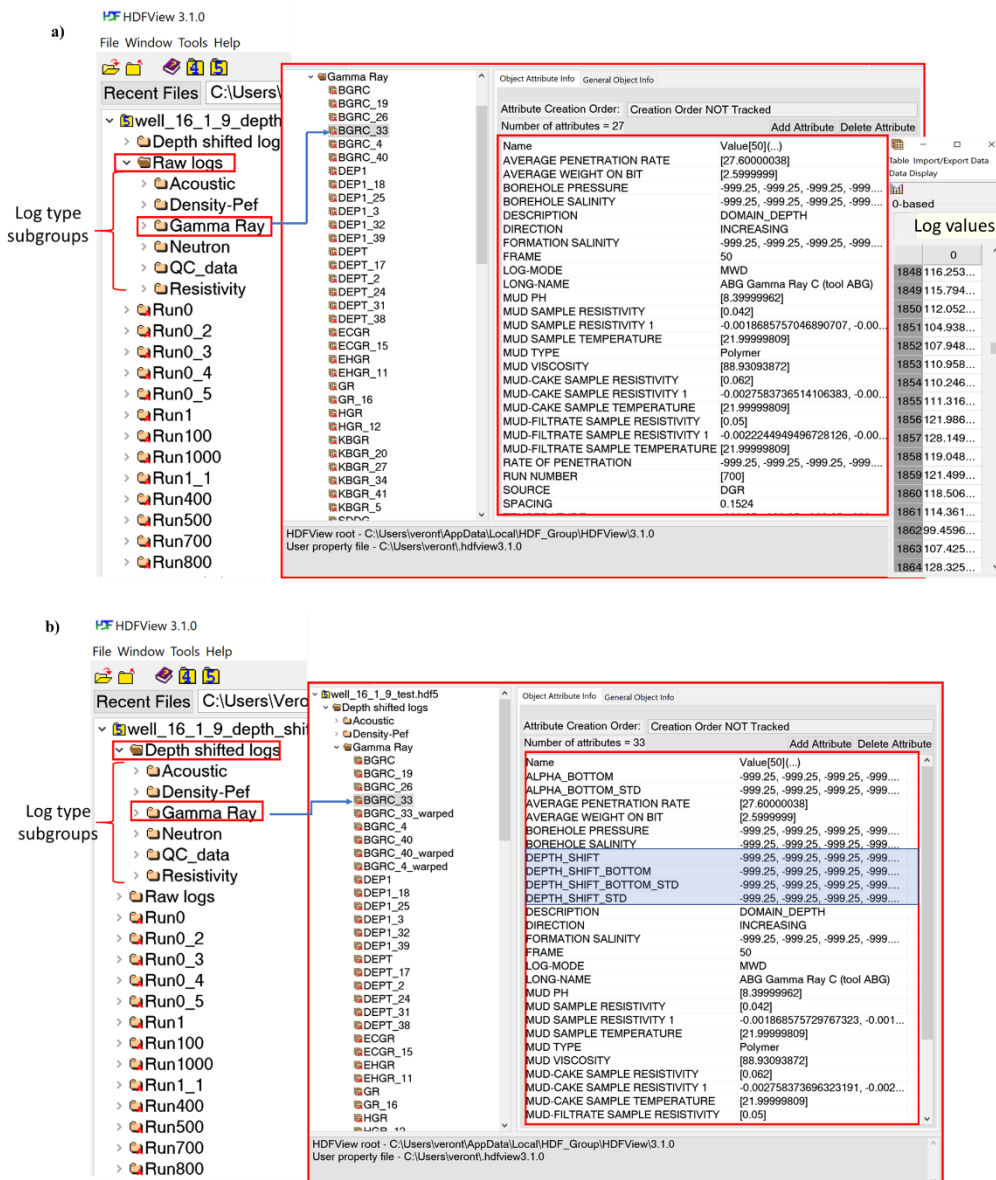


Fig. 3- Database visualization via HDFView for well 16/1-9; a) Example of the database after raw data selection process, on the left-hand side is the new folder's hierarchy (Raw logs) and on the right-hand side all the gamma ray logs and their corresponding depth values from all runs are displayed. The red square indicates the metadata associated with BGRC log and further to the right their values; b) Example of the updated database after depth matching process, on the left-hand side is the new folder's hierarchy (Depth Shifted logs) and on the right-hand side all the gamma ray logs shifted and warped are displayed. The red square indicates the metadata associated with BGRC log and the new metadata values are highlighted in blue.

We implement this idea in Python using *h5py* and *dlisio* packages. The former is a pythonic interface to the HDF5 binary data format (Collette et al., 2019). The latter are Python packages written and maintained by Equinor ASA, which allows the reading of DLIS files.

Note that *dllisio* version 1.14 (used in this implementation) was not able to read files containing tape marks, for example, Halliburton DLIS files (E Hårstad 2019, personal communication, 24 October). To address this issue, we read the Halliburton DLIS files using a Matlab application and created an additional function to reformat the data to be placed into a HDF5 format. However, the newer version of *dllisio* e.g. version 2.1 has overcome this issue, thus it can be used for Halliburton DLIS files.

Index	Log 1	Log 2	Log 3	Log 4	Log 5	Log 6	Log 6	Log 7	Log 8	Log 9	Log N
0				NAN	NAN	NAN	NAN	NAN	NAN	NAN	NAN
1		Section 1		NAN	NAN	NAN	NAN	NAN	NAN	NAN	NAN
2				NAN	NAN	NAN	NAN	NAN	NAN	NAN	NAN
3											
4	NAN	NAN	NAN				NAN	NAN	NAN	NAN	NAN
5	NAN	NAN	NAN				NAN	NAN	NAN	NAN	NAN
6	NAN	NAN	NAN		Section 2		NAN	NAN	NAN	NAN	NAN
7	NAN	NAN	NAN								
8	NAN	NAN	NAN								
9	NAN	NAN	NAN								
.	NAN	NAN	NAN						Section 3		
.	NAN	NAN	NAN	NAN	NAN	NAN					
.	NAN	NAN	NAN	NAN	NAN	NAN					
M	NAN	NAN	NAN	NAN	NAN	NAN					

Fig. 4- Sketch of a Python dataframe containing all the existing logs available in a well under a specific category e.g. Gamma Ray LWD ordered according to their depth position along the borehole via global index. Colors (blue, green, and orange) indicate the depth sections with valid values in the well and grey color indicates the automatic filling of the null values, ensuring the correct positioning of the logs guided by the global index vector.

AUTOMATIC DEPTH MATCHING OF WELLBORE LOG DATA

Depth misalignments between different wellbore measurements such as LWD/MWD (Logging While Drilling/ Measurement While Drilling) and EWL (Electrical Wireline Logging) are quite common because of ignoring the depth data uncertainty. This uncertainty is the result of several factors such as the depth measurement system itself, calibration accuracy, calculation of environmental factors' corrections during the acquisition, and uncertainty calculations (H Bolt 2021, personal communication, 17 May). In most cases these depth differences might lead to in LWD/MWD logs placed at shallower depths than their EWL equivalent (Chia et al., 2006, Pedersen et al., 2006). For example, LWD data are acquired at a variable sampling rate, which is controlled by the drilling rate. In other words, LWD measurements are acquired in a time-driven mode. The depth assignment is based on the driller's depth which is basically the length of the drilling pipe (at surface conditions and under zero tension or compression) projected along the wellbore. The actual length of the pipe (and therefore depth of the logging sensors) depends on the applied weight on the bit (WOB) and the torque on

the pipe as steel is elastic. Also, different rig-states during the drilling process affects the pipe length in different ways adding several levels of complexity for the application of the proper corrections to determine the absolute measured depth also known as along-hole depth (AHD) (Bolt, 2019). These instantaneous driller's depths are stored with respect to time for later merging with LWD downhole data. On the other hand, the EWL depth measurements are known as the loggers' depth. This is based on the length of cable that has gone into the well. It measures continuous depth as the tool goes up and down measured either using cable length as defined by calibrated measure wheels or using magnetic marks and measure wheel interpolation (Bolt, 2016, Wilson et al., 2004).

Both driller's and logger's depths are prone to errors that in most cases are not accounted for in the correction workflows applied to raw log data directly in the field. For LWD logs we have the following correction types: pipeline stretch up to 5 - 10 m increase due to different weights on the bit, thermal expansion (up to 3 - 4 m increase), pressure effects associated with differences between circulation fluid pressure and annular fluid pressure (contributing to an increase of approximately 1 - 2 m), ballooning effects caused by the change in average pressure inside or outside the tubing string (generating errors of about 2 m) causing an extension of the pipe length, as well as an increase in the diameter of the pipe that tends to compensate for the increased length, among others (Chia et al., 2006, Theys, 1999). In addition to this, there are other factors affecting the length of drillstring depending on a given rig-state such as: changes in fluid composition, flow rate, mud pressure, cuttings volume, helical and spherical buckling, friction, buoyancy, along-hole friction factor, etc. Changes in the penetration rate (ROP) and WOB also affects the length of the drillstring. These to MWD measurements are defined by the movement of the travelling block as well the bit position, therefore there are many corrections associated with the LWD depth measurements. (Bolt, 2019). EWL logs can suffer from tool sticking. This is when the depth recording system keeps measuring the movement of the cable while the tool remains in the same depth recording the log property measurements against that erroneous depth measurement. Cable stretching (elastic and inelastic) is another correction that is already applied at the wellsite before delivering the DLIS file from the first logging pass. The current practice in the industry to correct for this effect are the log-down/log-up correction where the AHD difference between a point near hold-up depth (HUD) is seen during run-in-hole

(RIH) log-down and the pull-out-of hole (POOH) log-up is considered to be the stretch correction. Stretch charts is another methodology that is based on a **cross plot** of the surface tension against depth. The calculated elastic stretch correction considers the thermal expansion of the cable with the elastic stretch. However, sometimes the well path can be complex and that cable stretching correction somewhat simplistic. To mitigate some of the shortcoming and assumptions of the current procedures Bolt (2016) proposed a waypoint correction for cable stretching that use the cable head tension and the surface tension. He also proposed a correction for the stick-and-pull effects. The application of these methodologies could provide a more consistent AHD measurements with reduced difference between LWD and EWL (Bolt, 2016). **There** are also effects of pressure **and** thermal expansion of the cable, which often seems to be a negligible **correction**, therefore they are not always considered, **as well as** twisting and rotating effects (Sollie and Rodgers, 1994). Other factors affecting depth accuracy are associated with surface setup stability, tension distribution (friction, tool sticking, cable keyseating), human errors, and measuring wheel accuracy (Theys, 1999).

More detailed explanations of these common issues are presented by Wilson et al. (2004), Brooks et al. (2005), Chia et al. (2006), and Pedersen et al. (2006). They also showed how it is possible to reduce the initial depth misalignment/desynchronization of logs curves between LWD and EWL if proper correction models are used for each depth measurement system independently (LWD and EWL) to compute the AHD with their corresponding uncertainties having a true-along-hole depth (TAH). **In order words, AHD is equivalent to the observed depth with corrections, and the TAH is the AHD with the measured uncertainties.** These depth differences can be magnified when data acquisition is carried out by different contractors at the same well, since each company uses their own methodology for depth determination, as illustrated by Bolt (2016). As we mentioned earlier, our aim is to generate an automatic workflow to reduce the depth mismatching/desynchronization between well logs from different runs logging the same depth intervals, which are synchronized with respect to a reference depth (EWL suite of log is considered to be at the correct depth) and incorporated into our database. **Therefore, we unfortunately do not have a TVD's uncertainty that can be related to a next well, this issue is out of the scope of this work.**

We develop a Python-based prototype depth matching workflow that is founded on an analytical signal processing approach using classical **cross-correlation** and **cross-correlation** with a scaling factor. The latter approach allows simulation of stretching and squeezing effects. For comparison, we apply depth matching of logs using a DTW algorithm.

Cross-correlation and cross-correlation with an additional scaling factor

We treat our log curves as a deterministic signal (depth series or depth vector), thus we use the signal processing **cross-correlation** method to measure the similarity of two logs as a function of their relative displacement. We define a reference depth series EWL log as $X=(x_1, \dots, x_N)$ and a test depth series LWD log as $Y = (y_1, \dots, y_M)$. Their cross correlation, c , at depth lag $k=0,1,\dots, \|X\| + \|Y\| - 2$ is given by Equation 1:

$$c(k) = (X * Y)(k - N - 1) = \sum_{i=0}^{\|x\|-1} x_i y_{i-k+N-1}^* \quad (1)$$

where $\|X\|$ is the length of X , $N = \max(\|X\|, \|Y\|)$, and y^* is the complex conjugate of y (Scipy.org, 2018).

Our implementation is as follows: **Firstly**, we select a common depth window for each drilled subsection where both LWD and EWL are available across different log measurement types e.g. gamma-ray, resistivity, density, pef (photoelectric factor), neutron, and acoustics. This is necessary as we aim to obtain a single depth shift for each **cross-correlation** window for all the log types in a way that their metadata can be shifted accordingly. In other words, all data must be shifted to a common reference depth axis. This common reference depth is defined under certain considerations. For example, we assume that any depth mismatch between logs acquired in the same logging run, is negligible. Therefore, we can say for example, that EWL gamma ray and EWL density logs acquired during the same run are aligned with a tolerance of 2 ft and 4 ft if it is a vertical well or deviated well, respectively (Bateman, 1986). The same assumption is made for LWD logs. The common depth ranges and individual depth intervals for each log type or measurement are determined considering the ranges given by both LWD and EWL. However, the number of logging sections are given by the LWD. **In** other words, we identify the starting and stopping depth of all valid values (**log values different**

from -999.25) of LWD and EWL log types and runs, which then define each log type depth range. After obtaining these ranges we identify a common starting and stopping depth across all log types per run. Where the starting and stopping depths are defined by the log type which starts deepest and the log type which ends shallowest, respectively. Differences between starting and stopping depths across log types are associated with the sensor positions along the tool string.

Secondly, we select the pairs of logs to be used for the cross-correlation, and the reference log is defined as the best EWL (the first up suit of logs to be run in the borehole) environmentally corrected GR for the gamma-ray pairs or deep laterolog resistivity for the resistivity pairs, for example.

Thirdly, we preprocess the logs to fill missing data intervals and remove spikes. Missing data are replaced with interpolation or log reconstruction depending on how large the gaps are. The filling of the gaps is constrained to be less than 50 samples that is equivalent to 25 ft (≈ 7.62 m), and it corresponds to less than 1/3 of the cross-correlation window size. When gaps are larger than this constraint the log is discarded. However, this is a temporal edition of the data since the cross-correlation needs continuous signals and cannot handle not a number (NaN) samples, thus after computations the original data are retrieved. Other examples of preprocessing are filtering/smoothing and normalization standardization to compensate for resolution discrepancies between LWD and EWL, for example the LWD gamma ray log shows higher vertical resolution than its equivalent EWL (see Fig. 7). This might be due to differences in logging speed, where the LWD is acquired with lower speed than EWL increasing the statistics and number of samples that are average and assigned to a given depth, as well as differences in sensors e.g. dual gamma ray sensors versus single sensor tools. This preprocessing also contributes to alleviate possible noise, and range values discrepancies as a result of variation between tools, contractor processing flows and technologies, borehole conditions, and drilling fluids, etc. For example, different parametrization for environmental corrections and changes in the borehole environment can lead to significant variations in the log's patterns and their values. A common example is the GR log that in general show the same patterns but can present a constant shift in their values (higher or lower) from run to run due to mud type corrections e.g. KCL mud.

Fourthly, depth matching is performed in a sliding window of length 50 m. This window length was selected based on a sensitivity analysis of variability of the depth shift as a function of window length, which is proportional to the number of **cross-correlation** windows, as well as being based on suggestions from expert petrophysicists. **We test window length of 100, 50 and 25 m, respectively. The larger the window more uniform depth shifts are obtained, and global patterns of the logs are used to do the match. On the other hand, smaller windows are more affected by noise in the signals and the shallow depth of investigation logs tend to show depth shifts highly deviated from the general trend shown by deep depth of investigation logs.** This window length is chosen to satisfy the trade-off between matching both geological low frequency trends (**global and high lithological contrast signatures e.g. gamma-ray deflection between shale and clean limestones**) and high frequency details (**local and weak contrast signatures e.g. gamma-ray deflections in a sequence of interbedded shales and sand or shaly-sands**) for most log types. In addition to the depth matching computations, some quality control metrics are estimated before and after depth mismatch corrections for comparison purposes, e.g. Pearson correlation, Euclidean distance, and the proportion of trace energy predicted. For details of these metrics we refer the reader to Appendix A. Cross-plot and depth section profiles are also output for visual inspection and quality control of the results.

After individual shifts are obtained for each pairs of log type (gamma-gamma, density-density, resistivity-resistivity, etc.), they are analyzed in terms of their variability between **cross-correlation** windows and as a function of their depth of investigation of each sensor as **illustrated** in Fig. 5. This shows the general depth dependence of the depth shift (Fig. 5a) and helps to identify outliers. We establish that any depth shift value representing +/- 40 samples or more, which is here equivalent to 20ft (~6 m), will be treated as an outlier, and therefore its weight will be set to zero. **However, if there are clear limits on the depth data value uncertainty given by operator companies for specific depth sections along the borehole, the user can decide on stricter depth shifts range to identify outliers.** Based on this, the user can **also** assign weights for each sensor giving higher weights to more reliable tools measurements or the ones less affected by borehole conditions (e.g. gamma ray and resistivity attenuation in this case) and compute a weighted average and standard deviation (uncertainty) in the depth shift, thus obtaining a single common depth shift across log types.

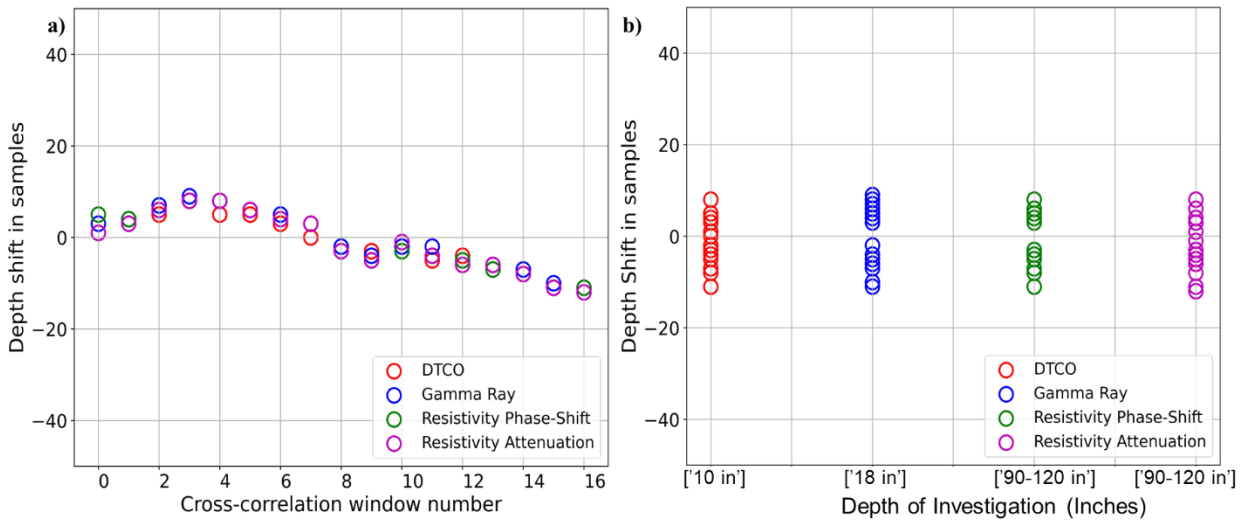


Fig. 5- Example of depth shift variability cross-plot for well 16/1-21S, drilling section 1; a) Depth shift variability in samples per cross correlation window; b) Depth shift variability as a function of sensor depth of investigation. The color code identifies each log type/sensor and the black arrow identifies anomalous depth shift values.

Fifthly, we apply the depth shift to all well log types together with log reconstruction. The latter approach considers both top and bottom log section (tails) that were excluded from the common window selection. These tails are given the shifts applied to the uppermost and lowermost cross correlation window within a log pass, e.g. the depth shift is held constant within the tails. The bottom of the log might for this reason shows a strong mismatch and deeper depth position than it should due to accumulated depth shifts applied along the whole wellbore section. To address this problem, we consider a cross correlation approach that includes stretching and squeezing effects through an additional scaling factor α (that represents a proportionality quantity between the length of the reference log (EWL) and the shifted log (LWD)). For instance, when $\alpha = 1$ a simple bulk shift is carried out, $\alpha < 1$ implies stretching of the shifted log, whereas $\alpha > 1$ implies squeezing.

The scale factor adds an extra degree of complexity to the cross-correlation computation as each cross-correlation must be performed as many times as there are α values. This allows the generation of contour maps of cross-correlation coefficients as a function of depth shift (ΔZ) and scaling factor α (Fig. 7). The α range is limited to $0.75 \leq \alpha < 1.25$, which is equivalent to a maximum stretching or squeezing of about 20 ft (~ 6 m). The

best α - ΔZ pair is the one that has the highest correlation value closest to 1. This pair is selected for correction of the data. Similarly, as for the common window depth matching, we attempt to find a single α - ΔZ pair for all log types that have bottom tails such as gamma-ray, density, pef., neutron, and resistivities. The acoustic logs are often positioned at the top of the tool string; hence they do not have tails at the bottom of the common depth window, the opposite is true for the gamma rays or resistivity logs (as it is the case) which are located right after the drilling bit. See a general example of a typical borehole assembly (BHA) in Fig. 6. The common α - ΔZ pair is computed following the same procedure as before via weighted average constrained by maximum values of ΔZ not larger than ± 10 samples (5 ft \sim 1.52 m) and $\alpha \geq 1$ (only squeezing effect is considered). The final step is the application of the bottom tails' correction and reconstruction of the final log. We assess the quality of the final depth matched logs by visual inspection and with the previously mentioned metrics. The final corrected log curves are then denormalized and reinserted into the database under a group called "Depth Shifted Logs". Their corresponding metadata are also shifted when applicable and included into the database. Notice that the depth shift values are also included as metadata.

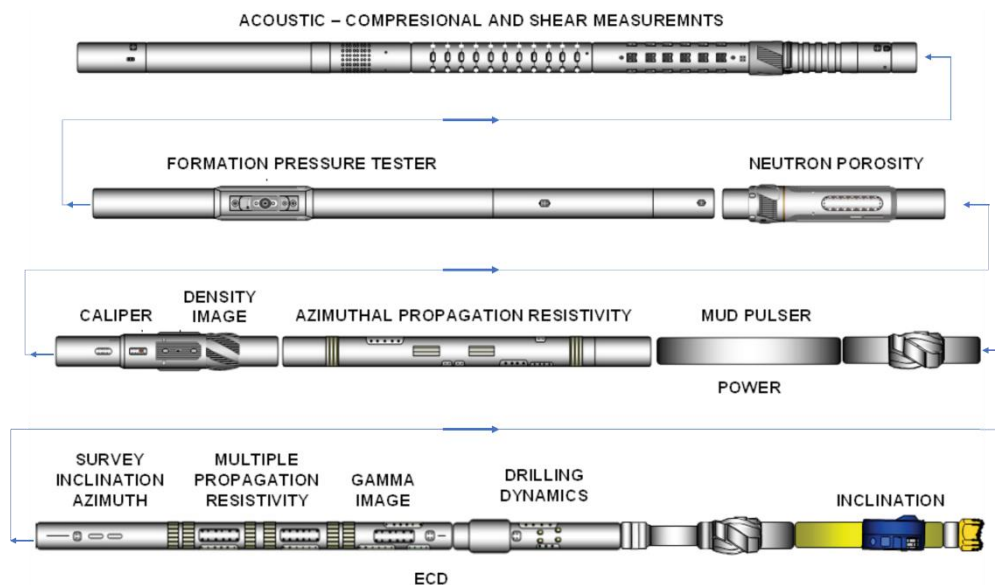


Fig. 6- Schematic diagram of a typical borehole assembly (BHA) with the LWD/MWD sensors. Modified and taken from Klotz et al. (2008).

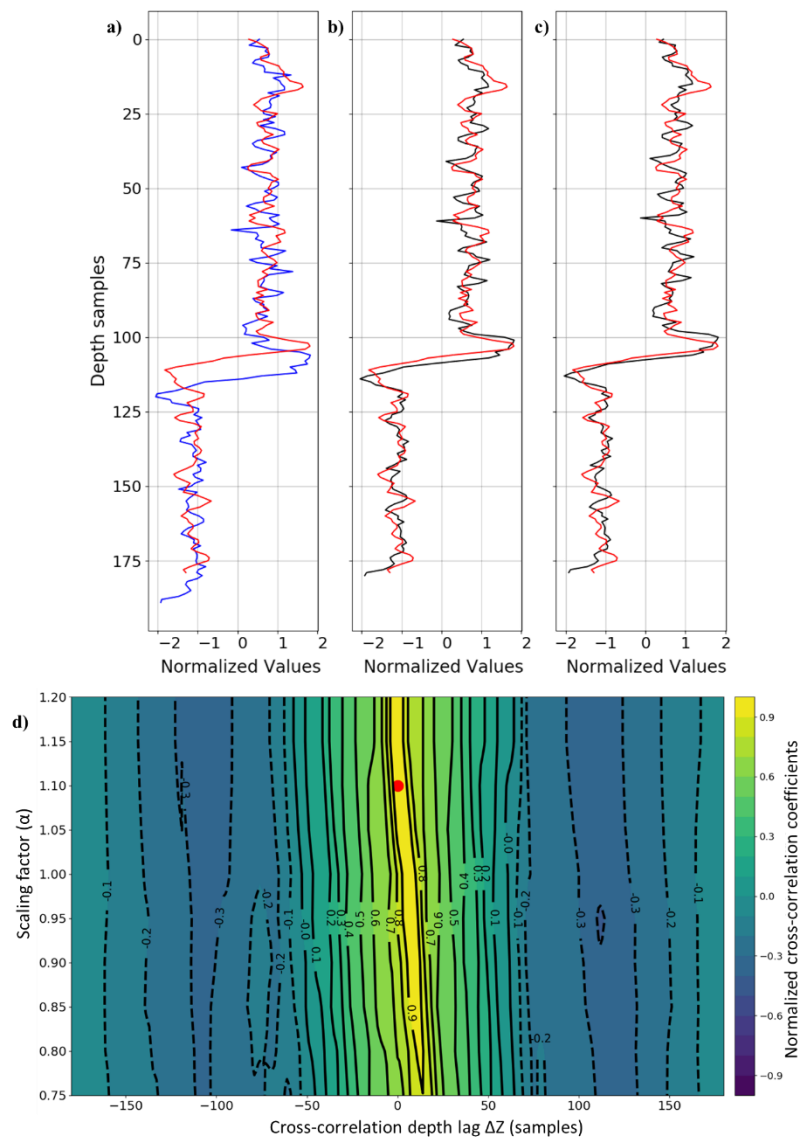


Fig. 7- Depth matching at the bottom tail via cross correlation with scaling factor example for well 16/1-9 gamma ray logs: a) Gamma ray logs before correction, blue LWD (test) and red EWL (reference); b) Gamma ray logs after squeezing process with $\alpha = 1.1$, black LWD (test) and red EWL (reference); c) Gamma ray logs after squeezing plus shift correction with $\Delta Z = 1$, black LWD (test) and red EWL (reference); d) Contour map of the cross correlation coefficients as function of ΔZ and α , the best $\alpha - \Delta Z$ pair is indicated with a red dot, and ΔZ represents the depth shift in number of samples.

Dynamic time warping (DTW)

DTW is a well-known technique used to find the best alignment between two time series under specific constraints. It provides a distance measure as well as the warping path that optimally deforms the test series to resemble the reference. Therefore, it can be used as a similarity measure between two series. This deformation

addresses the possible nonlinear relationship between signals, as well as, stretching and squeezing effects. However, it is important to avoid overfitting during the optimization process since this can lead to unrealistic results and excessive distortion of the original signal (Anderson and Gaby, 1983). One potential problem is that DTW may also change the intensity in the signal, not only correcting for shifts in the depth position.

The DTW algorithm can be described by assuming that we have two logs that need to be depth matched. Then we define the test log as $X=(x_1, \dots, x_N)$; and a the reference log as $Y = (y_1, \dots, y_M)$, where the indexing of X is $i=1, \dots, N$ and Y is $j=1, \dots, M$. It is also assumed that the dissimilarity distance d is given by a non-negative function f at each pair x_i and y_j as defined in Equation 2 (Giorgino, 2009).

$$d(i, j) = f(x_i, y_j) \geq 0 \quad (2)$$

The *Euclidean* distance is commonly used as a dissimilarity measurement along the warping path $\varphi(k)$, $k=1, \dots, Z$ that is, expressed as $\varphi(k) = (\varphi_x(k), \varphi_y(k))$ the warping functions φ_x and φ_y remap the time/depth indices of X and Y , respectively. **With** these elements in place, we can compute the average accumulated distance between each pair of points x_i and y_j :

$$d_\varphi(X, Y) = \frac{\sum_{k=1}^Z d(\varphi_x(k), \varphi_y(k)) m_\varphi(k)}{M_\varphi} \quad (3)$$

where $m_\varphi(k)$ is a per-step weighting coefficient and M_φ is the normalization constant that ensures that all of the accumulative distances can be compared regardless of the warping path (Giorgino, 2009). Several constraints are imposed within the algorithm to compute a φ that avoids undesirable solutions, for instance, end point constraints, local and global path constraints, axis orientation, and local distance measurements, as indicated by Anderson and Gaby (1983). The main idea of DTW is to find the optimal path that gives the minimum global dissimilarity $D(X, Y)$ or DTW distance by minimizing the cost function $d_\varphi(X, Y)$ (Giorgino, 2009):

$$D(X, Y) = \min_{\varphi} d_\varphi(X, Y). \quad (4)$$

We include DTW as an algorithm option in our prototype depth matching workflow, as well as cross correlation, since it is relatively fast, even though it has several pitfalls when it comes to generalization in the context of our application. For its implementation we use the *dtwdistance* package in Python (Meert, 2018). For example, each type of log will have their unique warping path that cannot be compared with the others, hence it is not possible to propagate **those depth shifts** to the sharing metadata (e.g. mud resistivity log) either to other logs of the same type (e.g. deep and medium resistivity logs). As an example, if we **depth match** bulk density, we need to compute two new warping paths to **depth match** for long and short spacing densities, respectively. **Moreover**, the application of the warping has fewer steps than those required for the **cross-correlation** process, as can be seen from Fig. 8.

For depth matching using DTW, first the data are selected from the “Raw logs” folder of the database (HDF5 file). Second, we use the individual depth range for each well log type, in contrast to when using the **cross-correlation**, where we must constrain our computation to a single common reference window. This is due to the uniqueness of the warping process for each individual log; therefore, we can skip that step. Similarly, we select a reference log (EWL) and a test log (LWD) of the same type e.g. gamma-gamma, resistivity-resistivity pairs and so on. Both are pre-processed by filtering/normalization before they are used in computations. **However, the filtering is not strictly necessary when we use DTW, we apply the filtering in this work to compare with the cross-correlation results.** We predefine the tuning parameters after exhaustive testing **for window size, penalty, and the relaxation parameter.** From where we observe that the most relevant parameter controlling the quality of the matching is the penalty term by regulating the degree of signal distortion as shown in Fig. 9, **we select a value of 2 for this terms that seems to show a good compromise between the resulting depth matching and the degree of signal distortion.** This is important to avoid perfect log alignments at expenses of obtaining an overfitted and highly distorted signal. **The window size, on the other hand, has significant impact on the computing time of the distance matrices, therefore the warping process itself, and the maximum shift allowed.** We select a window size of 300 and 50, where the only difference in the results is the execution time of the process. **The relaxation parameter (PSI) ignores the number of start and end points in the signal if this leads to a shorted distance in our case this parameter does not affect substantially the depth matching process, hence we**

select to keep the default values $PSI = 0$. For details of the selected parameters see Appendix B. The results are evaluated via visual inspection and quantitative metrics as for the **cross-correlation**. Finally, the warped logs are denormalized and incorporated into the database as a warped version under the “Depth Shifted Logs” group as an additional available log version. Fig. 8 shows the depth matching workflow for both options **cross-correlation** and dynamic time warping where we can see their interaction with the database. The advantage of the hierarchical structure is that makes easier the searching and organization of the data, therefore via Python coding we can select the target logs to be input in our proposed workflow. After the logs are depth matched the updated versions are retrieved into the database under the corresponding group/folder (Depth Shifted Logs).

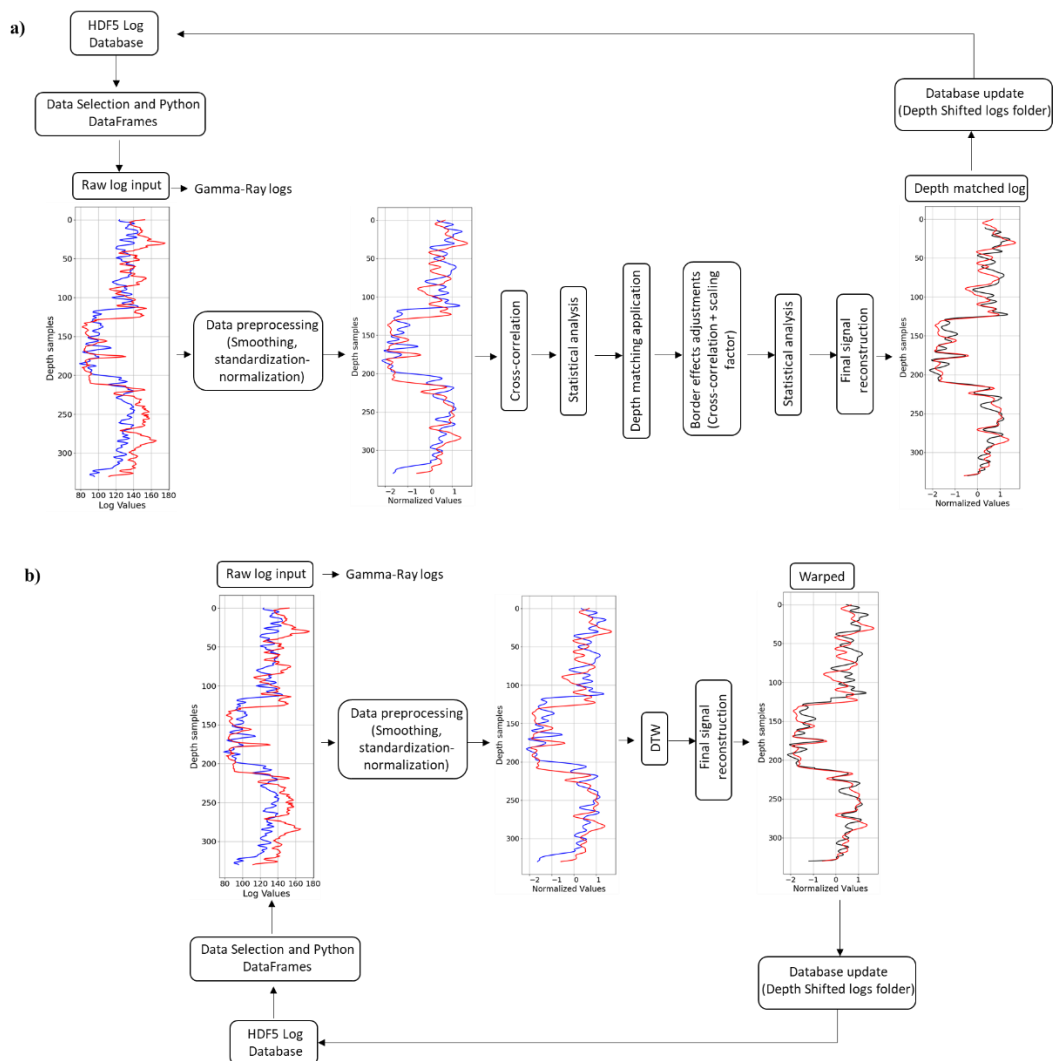


Fig. 8- Schematic diagram of the proposed depth matching workflow integrated with the log database (HDF5 file) for gamma ray logs. Solid line blue, red, and black represent the LWD log before depth matching, the reference EWL log, and the LWD log after depth matching, respectively: a) Depth matching process via cross-correlation; b) Depth matching process via DTW.

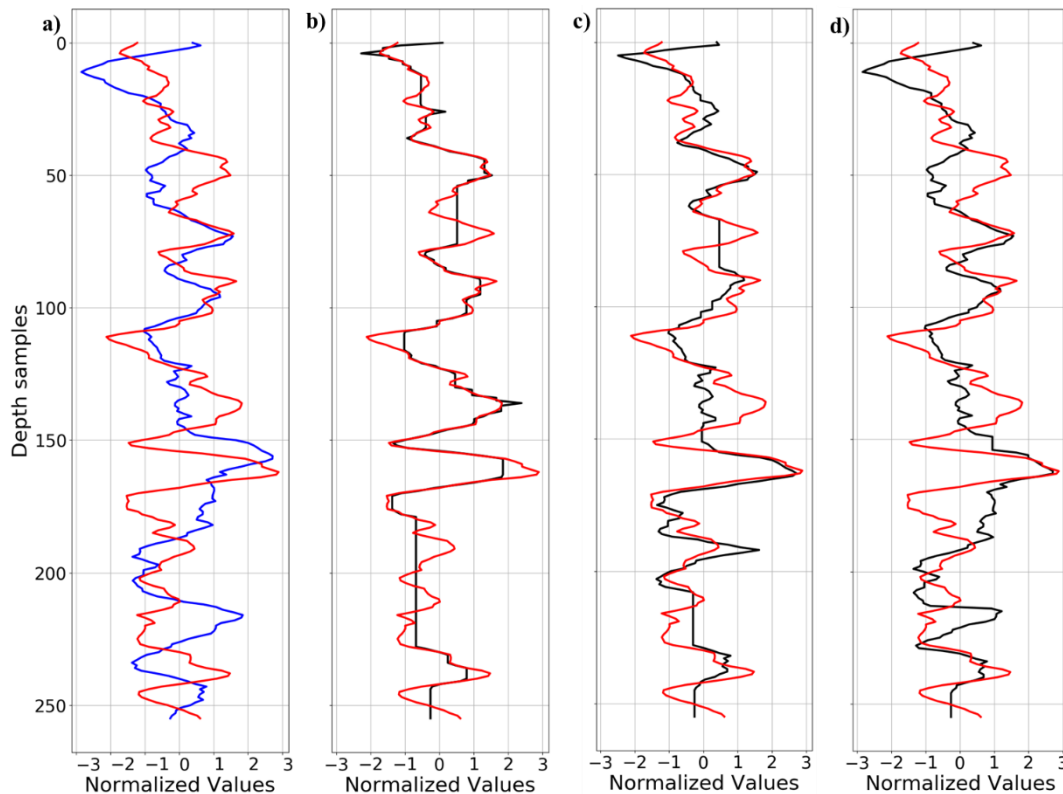


Fig. 9- DTW tuning parameter test for penalty values, example in Gamma ray logs for well 16/1-9. Solid lines (red) indicate the reference log (EWL measurement) and solid lines (blue and black) indicate the test log (LWD measurement) before and after depth matching, respectively where: a) Gamma-ray logs before depth matching with a Pearson correlation=0.198; b) Gamma-ray logs after depth-matching via DTW, penalty=0, warping distance =10.30 and Pearson correlation=0.929; c) Gamma-ray logs after depth matching via DTW penalty=1, warping distance =14.49 and Pearson correlation=0.772; d) Gamma-ray logs after depth matching via DTW penalty=2, warping distance =18.73 and Pearson correlation=0.423.

RESULTS

We implemented Python code for generating a structured database as a HDF5 file integrated with the depth matching workflow in two wells as a prototype test. These wells are key to model the Ivar Aasen field in the Norwegian North Sea. Example results are shown in Fig. 10 and Fig. 11. Note that these two wells have very different drilling planning, process, and amounts of data, and acquisition contractors. Well 16/1-9 was drilled with the drilling services of Halliburton in 2008, therefore the LWD/MWD data were also acquired by the same company, while the EWL data was acquired by Schlumberger. Well 16/1-21S was drilled with the drilling services of Schlumberger in 2015 and both LWD/MWD and EWL data were acquired by the same company.

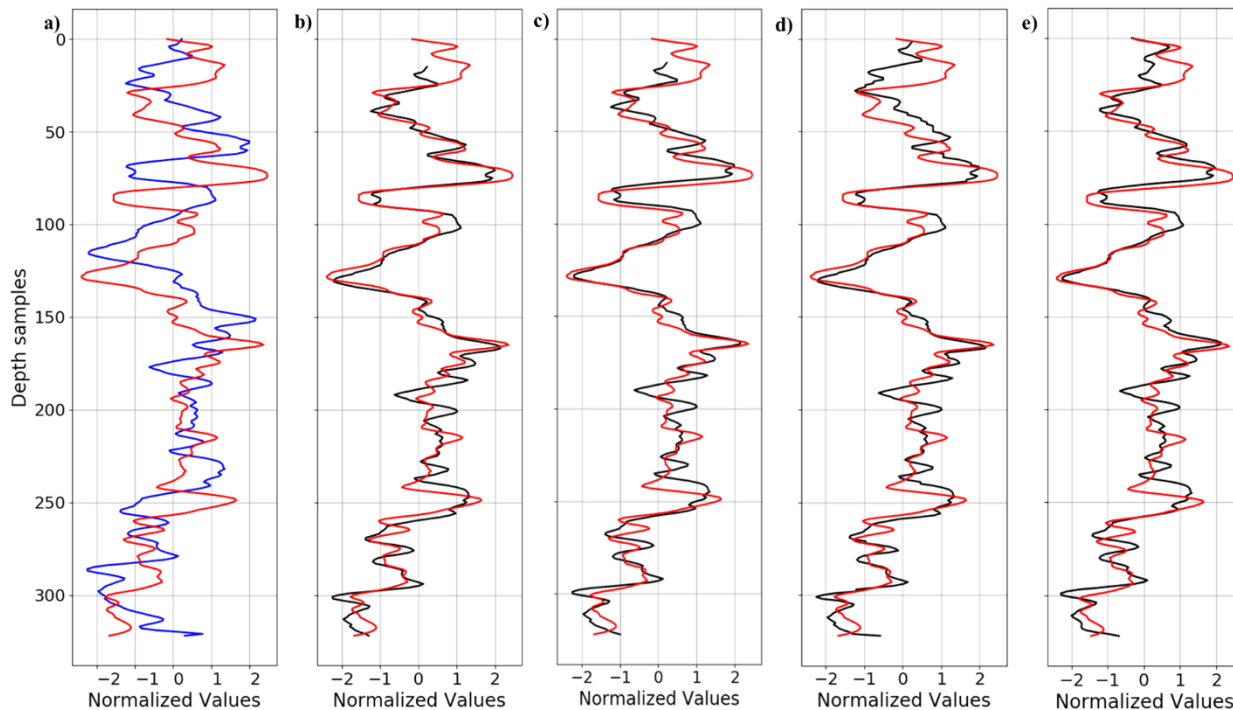


Fig. 10- Depth matching profile results for Gamma-ray logs from well 16/1-9 section 2 window 3. Solid lines (red) indicate the reference log (EWL measurement) and solid lines (blue and black) indicate the test log (LWD measurement) before and after depth matching, respectively where: a) Gamma-ray logs before depth matching; b) Gamma-ray logs after depth-matching via **cross-correlation** computed with Gamma-ray logs only (-15 depth sample shift); c) Gamma-ray logs after depth matching via **cross-correlation** computed as weighted average across all log types including gamma ray, acoustic, neutron porosity, density, and resistivity (-13 depth sample shift); d) Gamma-ray logs after depth matching via DTW with a warping distance = 12.778; e) Gamma-ray logs after manual depth matching performed by a petrophysicist.

From Fig. 10, we can observe the result of using a single **cross-correlation** window and data from well 16/1-9 where **misalignments** exist between gamma ray measurements acquired while drilling and after drilling using wireline tools. After the data are **depth matched** using both algorithms there is a substantial improvement in the alignment of the signals, as well as increased and reduction in their Pearson correlation and Euclidian distance, respectively. Significantly, Fig. 10c shows the **cross-correlation** results after applying a weighted average bulk shift of -13 depth samples (6.5 ft ~ 2.0 m), which differs slightly from the bulk shift computed only from the gamma ray pair, that is -15 depth samples (7.5 ft ~ 2.3 m) as shown in Fig. 10b . The **log** shown in Fig. 10c, will be the final **depth matched** log since we aim to have a common depth reference across all log types so that we can also match the metadata. On the other hand, Fig. 10d shows the results obtained by DTW with an optimal warping distance of 12.8 samples. The first 75 samples show the biggest differences in the depth

matching between algorithms. Both **cross-correlations** perform similarly except for the difference of two samples in the depth shift that is easy to see at the start of the log segment. In contrast, DTW induces a stretching effect trying to compensate for the shifting of the signal downwards, leading to poorer matching in the shallow part. Further down in the section approximately from depth samples 75 to 324 all three results are quite similar. For sake of completeness we present in Fig. 11e the result of a manual depth matching of the LWD log carried out by a petrophysicist (ground truth), we observe that this solution is very similar to the results given by our proposed workflow visually and quantitatively.

Fig. 11 shows an example of another way to do a quality control of the depth matching results. This is to compute a least-squares regression line between the signals and estimate the coefficient of determination R^2 . This can be used as an additional metric quality control. **In this case, we would expect a 45-degree regression line if our data are error free, if there are no tool setting parameters, and borehole condition differences. Even though this is not the case, we can see that after depth matching the regression line shows a slope quite close to 45 degrees and that the data align along a straight line. In contrast, the data before depth matching show a random behavior, and the regression line is closer to the horizontal. In addition, we see in dark red and light blue the 95% confident interval of the regression lines (before and after depth matching, respectively), which reflects the uncertainty of the fitted line.** Table 1 summarizes the values of the different metrics used to assess and compare the performance of the depth matching algorithms. This shows quite promising results for both methods compare to the mismatched data and the manual depth shifted data.

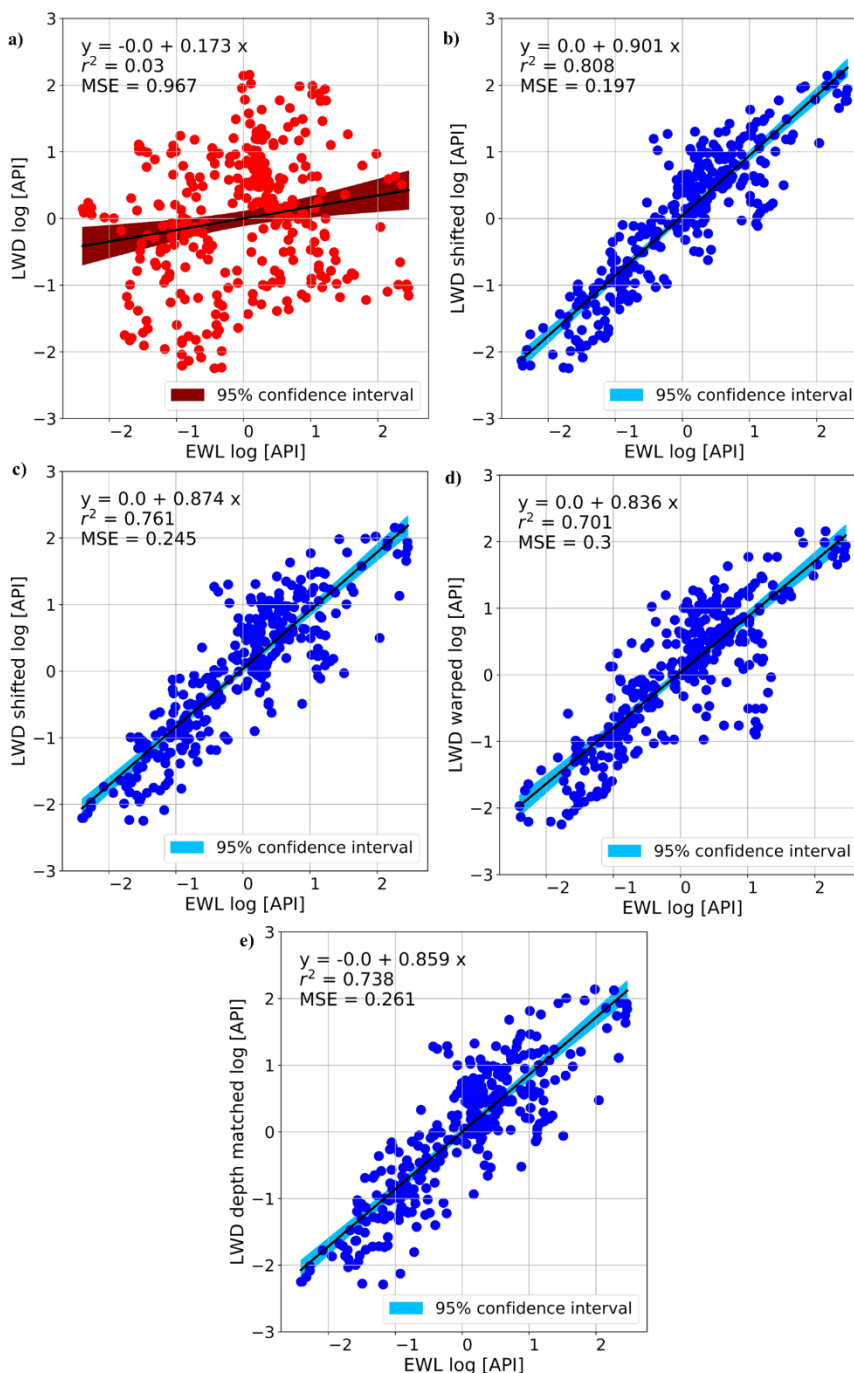


Fig. 11- Gamma ray logs interval normalized values from well 16/1-9 cross-plots before and after depth matching, with least-squares regression lines and their corresponding 95 % confidence interval. Solid line (black) is the least-squared regression line best fitting LWD logging plotted against EWL logging. All log values are normalized where: a) Cross-plot of gamma-ray logs before depth matching; b) Cross-plot of gamma-ray logs after depth matching via cross-correlation computed on gamma-ray logs only (-15 depth samples shift); c) Cross-plot of gamma-ray logs after depth matching via cross-correlation computed as weighted average across all log types including gamma ray, acoustic, neutron porosity, density, and resistivity (-13 depth samples shift); d) Cross-plot of gamma-ray logs after depth matching via DTW with a warping distance = 12.8 samples; e) Cross-plot of gamma-ray logs after manual depth matching performed by a petrophysicist.

Table 1-Algorithms Performance Based on Different Metrics for Depth Matching Assessment in Well 16/1-9 Section 2 and Window 1

Metrics	No Correction	Cross-correlation (Bulk-shift)	Cross-correlation (Weighted Bulk-shift)	DTW	Manual depth shift (Petrophysicist)
Pearson Correlation	0.17	0.90	0.87	0.84	0.86
Euclidean Distance	23.08	7.81	9.02	10.26	9.53
Proportion of Trace Energy	-0.65	0.81	0.74	0.67	0.72
R ²	0.03	0.82	0.76	0.70	0.74

A second example of the depth matching is shown in Fig. 12, which depicts a comparison of the depth matching results obtained by our proposed algorithm via **cross-correlation** (weighted average bulk-shift) and the results obtained by manual depth matching done by a petrophysicist. This example shows that our method suggests similar depth shift improving substantially the correlation and predictability between the logs, and reducing the Euclidean distance see Table 2. Even though the matching is significantly better than the original log position, below 110 depth samples approximately (blue shading zone) our method is not able to produce optimal results. **In contrast**, we see that the manual depth matching is showing a better solution. This is an indication of **possible stretch/squeeze** effects that our cross-correlation method is not able to deal with, being a limitation of our method. **The manual adjustment gives better results since the petrophysicist can manually select freely the number of key data points from the LWD log to be matched with the reference EWL and make the pertinent adjustments stretching and squeezing the signal. In contrast, the cross-correlation finds the depth lag at which the correlation between the signals is the highest by displacing one signal respect to the other one, in this case the displacement is constant value applied to all the data points within a window.**

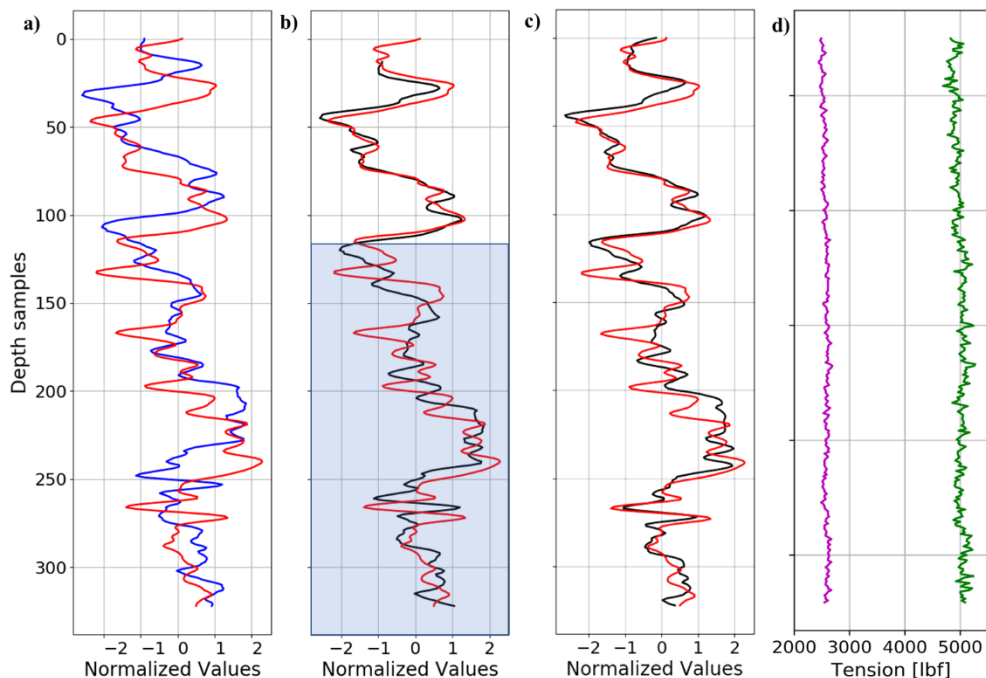


Fig. 12- Depth matching profile results for Gamma-ray logs from well 16/1-9 section 2 window 1. Solid lines (red) indicate the reference log (EWL measurement), solid lines (blue and black) indicate the test log (LWD measurement) before and after depth matching, respectively where: a) Gamma-ray logs before depth matching; b) Gamma-ray logs after depth matching via **cross-correlation** computed as weighted average across all log types including gamma ray, acoustic, neutron porosity, density, and resistivity (-13 depth sample shift); c) Gamma-ray logs after manual depth matching performed by a petrophysicist; d) **Surface tension (green) and cable head tension (magenta) these two logs are used as possible indication of stretch/squeeze zones. Blue shading box indicates the zones that required a dynamic depth shift (stretch/squeeze).**

Table 2-Algorithms Performance Based on Different Metrics for Depth Matching Assessment in Well 16/1-9 Section 2 and Window 1

Metrics	No Correction	Cross-correlation (Weighted Bulk-shift)	Manual depth shift (Petrophysicist)
Pearson Correlation	0.33	0.76	0.87
Euclidean Distance	20.76	12.32	9.05
Proportion of Trace Energy	-0.34	0.51	0.75

The cross-plots in Fig. 13 shows the clear benefit of applying a robust depth matching workflow to logs **before** any petrophysical or rock physics analysis and interpretation, as was pointed out by Zangwill (1982). In Fig. 13a, we see a cross-plot of density against neutron porosity before any depth corrections. Only the high gamma ray lithologies (> 100 API) can be discriminated from the rest, and those with medium and lower values (20 < GR < 100, and GR < 20 API) do not follow any distinctive trend. **Once** the depth correction is applied, we

can see a better trend and relocation of the data suggesting clearer lithological zones based on the gamma ray values.

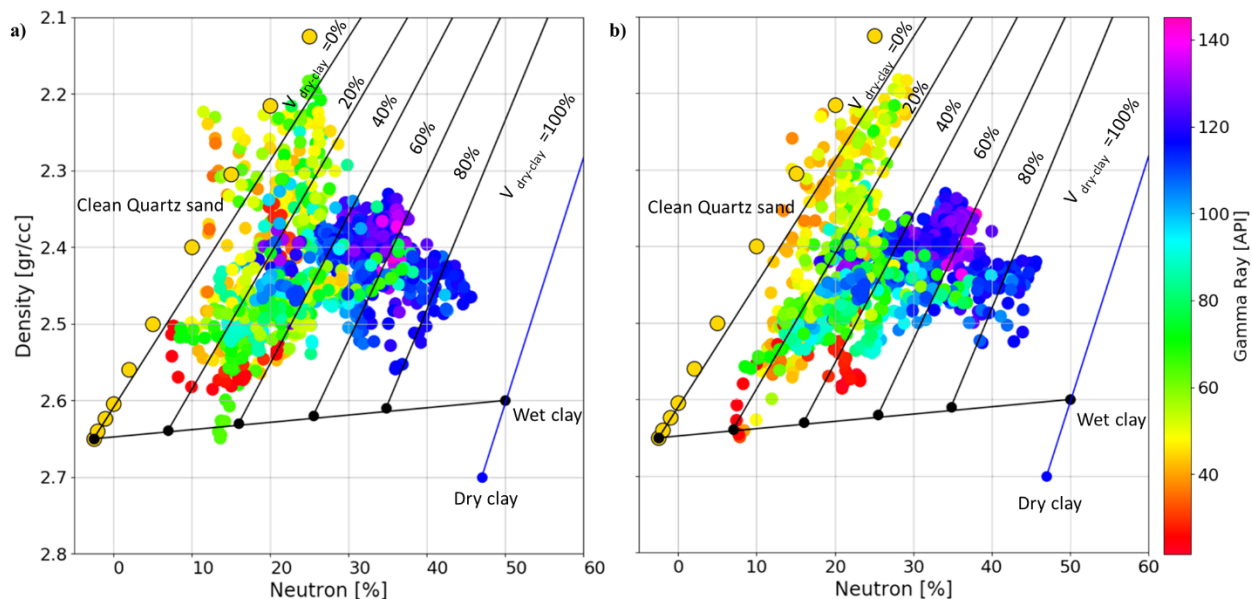


Fig. 13- Density (LWD/MWD) vs Neutron (EWL) cross-plot for well 16/1-21S at the deepest section, of well 16/1-21S from 7960 ft up to 8551.5 ft (2426.82 – 2607.16 m MD): a) Cross-plot before depth matching; b) Cross-plot after depth matching via **cross-correlation** with weighted average of all logs. Gamma-ray values (API) are shown by color. Yellow dots represent clean quartz sand with variable porosity, black dots represent calculated wet clay points, and blue the dry clay point all of these are theoretical values.

DISCUSSION

Our prototype implementation of the HDF5 format to build a structured well databases for wells 16/1-9 and 16/1-21S allows a wide range of new possibilities since it is **open-source** software and an **open-source** format with a high level of versatility, allowing easy and quick access to all data acquired in a hierarchical structure. It enables a continuous expansion of the database integrating in a single well pre-processing workflow as we show in this work (automatic depth matching). In tests, using a CPU: Intel® Core™ i9-8950 HK @ 2.90 GHz; RAM: 32 GB, we roughly estimated the computational cost of generating the structure database for the two wells. **These** findings are shown in Table 3. Here we see that it is possible to generate readable and easy to use databases in times ranging from minutes to a few hours, depending **on** the complexity of the drilling plan

and number of logs in a well. However, this effort is worthwhile for access to all the data and to facilitate better analysis and quality assessment. Even though this execution times are not optimal now, and one might think that also the storage of these files can be an issue. There is room for **improvement** using additional features offered by the HDF5 format. For instance, there exist options for chunking and compression for storage purposes. This means that the dataset can be created with HDF5's chunked storage layout by dividing the data into regular size blocks, which are stored in a way that there is not specific order and are indexed using a B-tree. In addition, we can apply filter pipelines into the chunked datasets this will apply transparent compression and decompression (Collette et al., 2019). In other words, the data are compressed during writing and decompressed during reading. Besides that, parallelization programming by implementing our database workflow in a graphics processing unit (GPU) could be considered to reduce substantially the processing times.

Table 3: Execution Times for Well Database Generation

Well	Total # of logs	Execution time (min)
16/1-9	1113	31.52
16/1-21s	6943	127.00

For the depth matching process, we observed superior results from **cross-correlation** compared to DTW even though the difference between these two are not significant, around to both visual inspection tools and numerical metrics. In most of the cases, the measured Euclidean distances were reduced substantially by approximately 66% for the best case via cross correlation (gamma-ray pairs only) and by 55.58% for DTW. The Pearson correlations were increased by 73 and 66%, respectively. Similarly, we observe higher values of R^2 after depth matching corrections for the three cases, where we have increases of about 78 and 67 % for **cross-correlation** and DTW, respectively. The proportion of the trace energy or predictability (PEP) also gives consistent results with the other metrics. In this case, we have a negative value of **-0.65** before depth matching that becomes high positive value close to 1 after **depth matching**. PEP **was** introduced by White (1980) as a goodness of fit measure to evaluate the match between synthetic seismograms and seismic traces. It basically measures the proportion of the trace energy predicted by the synthetic seismogram. We adopt this metric to

evaluate the proportion of the energy of the reference log that is contained in the test log. Since both logs are measuring the same depth section, when they are aligned, they should be closely equivalent, and the opposite occurs when they are not. The negative value obtained when there is a strong misalignment indicates that the residuals between the reference and the test log are larger than the total reference log energy, therefore we could expect very low predictability or energy content in the test log.

Comparing our **cross-correlation** results with a manual depth shift performed by a petrophysicist we prove that similar results are obtained. The first example Fig. 12 shows that our proposed **cross-correlation** workflow produce slightly better metrics than the manual depth matching, for example a **Pearson** correlation equal to **0.87** and **0.86**, respectively. However, we also show that in zones where strong stretch/squeeze effect are present our method struggles to find an optimal solution in comparison with the manual work, but it still improves the overall matching visually and quantitatively with respect to the original well position (Fig. 12 and Table 2). This behavior occurs because **we are now** considering only bulk shift as first step of an automatic depth matching workflow.

Even though both approaches are relatively fast and simple to implement, the DTW is a more expensive process than the **cross-correlation** workflow when the number of processed curve increases. Table 4 shows the comparison in computational cost of implementing either **cross-correlation** or DTW as depth matching algorithm, for both wells, using the same CPU characteristics for testing as were used for the speed test of database generation. Execution time for DTW is higher than double the execution time for **cross-correlation** for well 16/1-9, and the execution time difference between the two wells is quite small when **cross-correlation** is used. This is because even though well 16/1-21S has six times as many logs as well 16/1-9 we only perform depth matching in a small subset of the logs, and from those only the LWD/MWD logs are processed. In this case, the number of relevant logs for this speed test is 26 in well 16/1-21S and 21 in well 16/1-9. However, for DTW, there is a significant increase in execution times for well 16/1-21S relative to both **cross-correlation** and DTW execution times in the 16/1-9 well, even though the difference in the number of curves processed is only 5. It is known that the DTW has time and space complexity of $O(N^2)$ which typically limits its use to small series of no more than thousands of samples (Salvador and Chan, 2004). This issue is also mentioned and

addressed by Hale (2013) in his implementation of DTW for use on seismic images. The time complexity can be reduced by using constraints on the length of the window, which limit the search for the optimal warping path within the constrained window. However, such window constraints only work if the warping path is close to linear and it passes through the diagonal of the cost matrix, otherwise the performance of the method will not be satisfactory (Salvador and Chan, 2004). In our case, the selection of a penalty=2 to avoid excessive distortions makes the warping path to be close the main diagonal of the cost matrix, hence we can reduce the window size from 300 to 50 samples. This improves the DTW execution times as shown in Table 4. From where we can see that DTW is faster than **cross-correlation** in well 16/1-9 and even though it is still slower than **cross-correlation** in well 16/1-21S the original time is reduced in approximately 1/3. It might be worth testing *FastDTW* python package that perform DTW with a multilevel approach using recursive projections of the warp path from a coarser to finer resolution and then updates it. This gives an approximation to the DTW solution and it can also run much faster for larger datasets. However, Salvador and Chan (2004) emphasized that this approach does not guarantee an optimal solution and additional research is necessary to improve the accuracy of this algorithm. For these reasons, **cross-correlation** yields reliable results in shorter times, thus increasing the efficiency of the workflow without compromising accuracy.

Table 4: Depth Matching Algorithm Execution Times per Well

Well	Depth Matching Method	Execution time (min)
16/1-9	Cross-correlation	10.56
16/1-9	DTW	28.38
16/1-9	DTW window size=50	8.98
16/1-21s	Cross-correlation	10.99
16/1-21s	DTW	64.20
16/1-21s	DTW window size=50	20.37

Cross-correlation also has several advantages that better fulfill our requirements based on the concept we want to develop and implement. To be more specific, the **cross-correlation** is a simple analytical process that allows full control of what the algorithm is doing. We also easily establish a weighted average to be applied to all the log types. This allows the metadata to be synchronized correspondingly. **As far as we are aware**, this is a feature that has not been considered in well log storage formats before, as far as we are aware. In contrast, the DTW even though it produces good results, acts as a shaping filter that is prone to overfitting the data if the

regularization parameters used during the optimization process are not tuned properly. This was demonstrated by Herrera and van der Baan (2014) who implemented DTW for tying well logs and seismic data. They emphasized that unconstrained DTW can achieve an optimal signal match, however, this may also lead to non-physical velocities and time-depth functions. The same applies for our case as it was shown in Fig. 9. Therefore, the parameter tuning stage is important. It also adds another level of complexity, user intervention and additional time to the process. We have constrained DTW to avoid perfect matching between the reference (EWL) and test (LWD/MWD) logs, resulting in a slightly lower performance than **cross-correlation**, and to speed up the process. After all, we are not aiming to transform the test log (LWD) **into** the reference log (EWL), we also want to preserve as much as possible of the original log retaining the inherent difference and just perform the log alignment as accurately as possible. Similarly, each pair of curves will have their own unique warping solution that cannot be standardized and applied to the metadata.

Anderson and Gaby (1983) and Hale (2013) showed that simple **cross-correlation** can yield good results providing that the reference and the test signal have similar patterns and the time difference between them is neither too large nor too rapidly varying. We also saw a few **cross-correlation** windows in which erroneous lags were determined due to the lack of distinctive patterns within the window. For example, zones containing only a single lithology type (shaly interval). In addition, we found poor matching performance in zones with large differences between LWD and EWL patterns, these were most presented in shallow depth of investigation sensor. Those might be associated with areas where the borehole conditions have changed significantly between runs, for example borehole enlargement and barite content in the mud, which deteriorates the pef signal making it unreliable. In the same way, these conditions affect the density even though the corrections have been made. Another case could be shallow or medium resistivity measurements in high porosity formations, where the drilling fluids can invade quickly the formation and patterns differences might be easily detected between LWD and EWL if considerable difference in resistivity exist between drilling fluids and formation fluids. Therefore, in these cases we should not expect sensible results. However, we alleviated this problem by imposing maximum and minimum acceptable depth shift values (**± 30 depth samples that is equivalent to ± 15 ft**) to detect outliers or unreasonable results and by introducing a weighted average into the final depth shift estimation. The need to

set these limits could be interpreted as disadvantage of the **cross-correlation**, as it needs more user intervention than DTW.

The results obtained from the density vs neutron cross-plots shown in Fig. 13 is a good example of the importance of depth synchronization or alignment when it comes to petrophysical analysis and interpretation which combines LWD/MWD and EWL data. These results come from the deepest section of well 16/1-21s, which is about 591.5 ft (180.34 m) thick. This section includes two geological groups such as the Viking and Hegre groups of the Norwegian North Sea. **The** Viking group consist of the Draupne (identified as source rocks) and Heather formations. The former is characterized by carbonaceous claystones with a very high radioactivity, low velocities and densities, and the latter is rich in silty claystones with some limestone stringers. On the other hand, the Hegre group in this well consists of the Skagerrak formation, which has interbedded conglomerates, sandstones, siltstones, and shales. In addition, this formation includes anhydrite, dolomites, and limestones (NPD, 2020). These distinctives lithologies can be **easily identified** on the depth corrected cross-plot where the shales and claystones after correction move toward high neutron porosity and low to moderate densities, falling in the range from 40 to 100 % volume of dry clay, whereas the cleaner sandstones with porosities about 20 and 25 % are well separated moving toward lower density values about 2.2 – 2.4 gr/cc suggesting possible hydrocarbon bearing sands that were proved in this formation at this depth interval via core analysis and fluid sampling tests. We also see that these reservoir sands have lower percentage of clay, less than 20 %. Similarly, very low gamma-ray values < 20 API, low neutron porosity < 10 %, and high density above 2.7 gr/cc can be associated with the dolomite, marls, and limestone stringers. In contrast, the same cross-plot before depth synchronization leads to misinterpretation and poor lithological discrimination.

CONCLUSION

We presented a novel database structure format optimized towards automation and machine learning-based approaches applied to well log data analysis. We suggested a hierarchical restructuring of the complex DLIS files to a more comprehensive and versatile HDF5 formatted file, as well as the estimated execution times for two wells from the Norwegian North Sea with different drilling planning strategy, acquisition contractors,

and numbers of logs. This fully automated database generation is done in either minutes or a few hours depending on the amount of data in a well. Shortening of workflow execution times is important for the oil industry to improve efficiency. Similarly, there is room for improvement in the research Python code, for code generalization and to speed up the execution times through parallel processing of the data by using GPU and reductions of files size without compromising the data itself via chunking and compression filters as HDF5 features, for instance. In addition, our database prototype proposal seems to fit with the Open-Source Data Universe (OSDU) vision, sharing the aim to organize and manage data in an innovative way that suits in the current digital transformation across different industries. Our hierarchical structure can be a starting point to explore new possibilities of data management.

We also compared two different algorithms for automated well-log depth matching of wells. We demonstrated the use of a few of these methods integrated into a single workflow. Considering that our main aim is to get better control of the data and simultaneously depth match the metadata, the traditional cross-correlation algorithm plus scaling factor (α) for the log tails is the best method applied here. This also provides the best results qualitatively (via cross-plots) and quantitatively (QC metrics) with good agreement among all metrics. DTW shows good alignments but at the same time, introduces some artifacts in zones with high stretching effects. Additionally, the non-uniqueness of the warping logs to each log types makes it unstable when estimating of a single depth shift that can be applied across all logs along with their metadata, which is one of the innovative features of our workflow. In addition, the cross-correlation approach outperforms with execution times around 1/3 when compared to those for the DTW providing that not window length constrains are applied, although, it required more user intervention and a more complex workflow than the warping. On the other hand, DTW can be speeded up when the warping path's searching grid is constrained, however, we showed that it will be more costly than cross-correlation whenever the number of log curves increases. We emphasized the importance of depth matching and the necessity of providing a quick and robust solution to this long-standing problem via automation by demonstrating the benefit of depth matching exemplified as classical log analysis and lithological interpretation.

Our new framework has been **prototype tested** in two **Norwegian North Sea wells**. However, the implementation of this automated database and workflow for more wells would allow us to improve the generality of the research Python code, as well as the robustness of the depth matching estimates and possible implementation of new metrics. Towards automation and reduction of user intervention we envisage several possibilities to improve our current proposal, for example a hybrid solution in which the **cross-correlation** workflow is run first, and a second run is performed via DTW. This will alleviate the issues of stretch/squeeze that the former cannot handle, and it will potentially simplify the proposed **cross-correlation** workflow by suppressing the need of applying a **cross-correlation** with a scaling factor to adjust the tails of the log section. Similarly, the usage of machine learning to replace the statistical analysis step from the **cross-correlation** workflow and to automatically select and adjust a window size for depth synchronization analysis will bring benefits in terms of automation. We will further evaluate the feasibility of applying this approach to a massive number of wells, potentially **significantly contributing** in reducing well log processing times and introducing a hierarchical organization of the data. We believe that better data management enables new possibilities for exploring, assimilate, and use all the data acquired in a wiser manner enables faster and better understanding of data quality, data measurement sensitivity and data mining. **Additionally, it would be valuable to give as an input suite of logs already referenced to a AHD and TAH that honor the operator requirements of quality, therefore the initial misalignment between LWD and EWL logs will be less and at the same time this will output depth matched logs aligned and referred to a more accurate absolute depth.**

ACKNOWLEDGMENTS

This research is part of **the** BRU21 – NTNU Research and Innovation Program on Digital and Automation Solutions for the Oil and Gas Industry (www.ntnu.edu/bru21) and **is** supported by AkerBP. We thank also NTNU-NPD-Schlumberger Petrel ready dataset for borehole data, and Andrew J. Carter for his suggestions for improving this manuscript. Additionally, we thank to the reviewers and the editor for all their constructive comments and suggestions that have helped to substantially improve this manuscript.

NOMENCLATURE

Abbreviations

AHD = along-hole depth

BHA = borehole assembly

DLIS = digital log interchange standard

DTW = dynamic time warping

EWL = electrical wireline logging

GPU = graphics processing unit

GR = gamma ray

HDF5 = hierarchical data format version 5.

HUD = hold-up depth

LWD = logging while drilling

MWD = measure while drilling

PEF = photoelectric factor

PEP = proportion of the trace energy o predictability

POOH = pull out of hole

RIH = run in hole

ROP = rate of penetration

TAH = true along-hole depth

WOB = weight on the bit

APPENDIX A SUMMARY OF METRICS USED FOR DEPTH MATCHING ASSESSMENT

Pearson correlation coefficient

The Pearson correlation coefficient, r , is often used to measure the degree of relationship between two variables assuming that there is a linear relation between them. Its values lie between -1 and 1, where a value of -1 implies perfect negative correlation and a value of 1 implies perfect positive correlation. Values equal to zero

or close to zero indicate that there is no linear correlation (Bulmer, 1979). The correlation coefficient is defined by the following equation:

$$r = \frac{\sum_{i=1}^n (x_i - \bar{x})(y_i - \bar{y})}{\sqrt{\sum_{i=1}^n (x_i - \bar{x})^2 \sum_{i=1}^n (y_i - \bar{y})^2}} \quad (\text{A-1})$$

where n is the sample size, x_i and y_i are the individual sample points of the depth series and \bar{x} and \bar{y} are the corresponding mean values for x and y .

Proportion of trace energy predicted

The proportion of trace energy predicted by synthetic seismograms also called predictability (P) was introduced by White (1980) as an additional output from wavelet estimation through matching. This concept is used as a goodness of fit measure to assess the reliability of a well-seismic tie. There are two terms that need to be defined, the trace energy, and the residual energy. The energy of a trace, TE that in our case is the reference log, is the sum of the squares of the amplitude of a segment of the time/depth series. See Equation (A-2). The residuals energy is the square of amplitude difference between the samples of a seismic trace (reference log) and its matched synthetic seismogram (test log) after depth shifting. See Equation (A-3) (White and Simm, 2003).

$$TE = \sum_{i=1}^n x_i^2, \quad (\text{A-2})$$

$$RE = \sum_{i=1}^n (x_i - y_i)^2, \quad (\text{A-3})$$

where n is the sample size, x_i and y_i are the individual sample points of the reference and test logs, respectively.

The predictability (P) is given by:

$$P = 1 - \frac{RE}{TE} \quad (\text{A-4})$$

Euclidean distance

Euclidean distance also known as the L_2 -norm is an alternative metric to measure the degree of similarity between time and depth series as given by Equation (A-5) (Herrera and van der Baan, 2014):

$$D_{euclid(x,y)} = \sqrt{\sum_{i=1}^n (x_i - y_i)^2} \quad (\text{A-5})$$

where $D_{euclid(x,y)}$ is the one-to-one Euclidean distance between the test (LWD/MWD) log x , and the reference (EWL) log y , the index i representing the individual sample points in each depth series.

APPENDIX B DTW PARAMETRIZATION

The *dtw.distance.dtw* function provides several options for addressing the complexity of DTW. For instance, even though the distance function has a linear complexity in space, in the time domain, the complexity is still quadratic. The most common approach to overcome this, is the use of a window that constrains the maximum shift allowed. Any shift larger than the window length will be rejected. This is a direct implementation of the global constraints widely used to speed up DTW e.g. the Sakoe-Chiba Band (Herrera and van der Baan, 2014). As well as the window length, we have three more parameters that trigger early rejection of some or all paths the dynamic programming explores (Meert W., 2018):

- **max_dist**: stop the computation if the distance is larger than this value.
- **max_step**: path searching steps cannot be larger than this value.
- **max_length_diff**: return infinity if the difference in length of the two series is larger than the given value.

There are two additional options that are considered as tuning parameters for the optimization process, in order words, they tune how the cost is computed (Meert W., 2018):

- **penalty**: penalty added to the distance if compression or expansion is applied (distortion).
- **psi**: relaxation to ignore the beginning and/or end of sequences.

We have used the following values for these parameters: window=50, max_dist=100, max_step=50, penalty=2, psi=2. Where the three first parameters are represented as the number of samples.

REFERENCES

Anderson, K. R., and J. E. Gaby, 1983, Dynamic waveform matching, *Information Sciences*, **31**(03), 221-242. DOI:[10.1016/0020-0255\(83\)90054-3](https://doi.org/10.1016/0020-0255(83)90054-3).

Bateman, R.M., 1986, Openhole log analysis and formation evaluation.

Bolt, H., 2016, Wireline Logging Depth Quality Improvement: Methodology Review and Elastic-Stretch Correction, *Petrophysics*, **57**(03), 294-310.

Bolt, H., 2019, Correction of Driller's Depth: Field Example Using Driller's Way-Point Depth Correction Methodology, *Petrophysics*, **60**(01), 76-91. DOI: [10.30632/PJV60N1-2019a7](https://doi.org/10.30632/PJV60N1-2019a7).

Brooks, A. G., H. Wilson, A. L. Jamieson, D. P. McRobbie, and S. G. Holehouse, 2005, Quantification of depth accuracy, Paper SPE-95611-MS presented at the SPE Annual Technical Conference and Exhibition, Dallas, Texas, USA, 9-12 October. DOI: [10.2118/95611-MS](https://doi.org/10.2118/95611-MS).

Bulmer, M. G., 1979, *Principles of statistics*, Courier Corporation.

Chia, C. R., H. Laastad, A. V. Kostin, F. Hjortland, and G. A. Bordakov, 2006, A new method for improving LWD logging depth, Paper 102175-MS presented at SPE Annual Technical Conference and Exhibition, San Antonio, Texas, USA, 24-27 September. DOI: [10.2118/102175-MS](https://doi.org/10.2118/102175-MS).

Collette A. and contributors, 2019, H5py: Documentation Release 2.10.0, <https://buildmedia.readthedocs.org/media/pdf/h5py/stable/h5py.pdf>, accessed 6 September 2019.

Equinor, 2019, Dlisio: Documentation Release 0.1. <https://buildmedia.readthedocs.org/media/pdf/dlisio/stable/dlisio.pdf>, accessed 4 October 2019.

Giorgino, T., 2009, Computing and visualizing dynamic time warping alignments in R: the dtw package, *Journal of Statistical Software*, **31**(07), 1-24.

Hale, D., 2013, Dynamic warping of seismic images, *Geophysics*, **78**(02), S105-S115. DOI: [10.1190/geo2012-0327.1](https://doi.org/10.1190/geo2012-0327.1).

Herrera, R. H. and M. Van Der Baan, 2014, A semiautomatic method to tie well logs to seismic data, *Geophysics*, **79**(03), V47-V54. DOI: [10.1190/geo2013-0248.1](https://doi.org/10.1190/geo2013-0248.1).

Kerzner, M. G., 1984, A solution to the problem of automatic depth matching, Paper SPWLA-1984-VV presented at SPWLA 25th Annual Logging Symposium, New Orleans, Louisiana, USA, 10-13 June.

Klotz, C., A. Kaniappan, A. K. Thorsen, E. Nathan, M. Jahangir, and L. Lie, 2008, A new mud pulse telemetry system reduces risks when drilling complex extended reach wells, Paper SPE-115203-MS presented at the IADC/SPE Asia Pacific Drilling Technology Conference and Exhibition, Jakarta, Indonesia, 25-27 August. DOI: [10.2118/115203-MS](https://doi.org/10.2118/115203-MS).

Le, T., L. Liang, T. Zimmermann, S. Zeroug, and D. Heliot, 2019, A Machine-Learning Framework for Automating Well-Log Depth Matching, *Petrophysics*, **60**(05), 585-595. DOI: [10.30632/PJV60N5-2019a3](https://doi.org/10.30632/PJV60N5-2019a3).

Liang, L., T. Le, T. Zimmermann, S. Zeroug, and D. Heliot, 2019, A Machine Learning Framework for Automating Well Log Depth Matching, Paper SPWLA-2019-S presented at the SPWLA 60th Annual Logging Symposium, The Woodlands, Texas, USA, 15-19 June. DOI: [10.30632/T60ALS-2019_S](https://doi.org/10.30632/T60ALS-2019_S).

Meert, W., 2018, Dynamic Time Warping (DTW), <https://dtaidistance.readthedocs.io/en/latest/usage/dtw.html#dtw-distance-measure-between-two-series>, accessed 15 July 2019.

Müller, M., 2007, *Dynamic time warping in Information retrieval for music and motion*, Springer, Heidelberg.

Munoz, A. and D. Hale, 2014, *Automatic simultaneous multiple-well ties*, Center for Wave Phenomena. Report, 788, 41.

Myers, C., 1980, *A Comparative Study Of Several Dynamic Time Warping Algorithms For Speech Recognition*, Doctoral dissertation, Massachusetts Institute of Technology.

Norwegian Petroleum Directorate (NPD), 2020, Fact Pages, <https://factpages.npd.no/en/wellbore/pageview/exploration/all/7529>, accessed 10 June 2020.

Norwegian Petroleum Directorate (NPD), 2019, Guidelines for reporting well data to authorities after completion "Blue Book", https://www.npd.no/globalassets/1-npd/regelverk/forskrifter/en/b_og_b_digital_rapportering_e.pdf, accessed 25 November 2019.

Pedersen, B.K., Constable, M.V. and Risbakken, J.K., 2006, Operational Procedures and Methodology for improving LWD and WL Depth Control, Kristin Field, Paper SPWLA-2006-XXX presented at the SPWLA 47th Annual Logging Symposium, Veracruz, Mexico, 4-7 June.

Salvador, S. and P. Chan, 2004, FastDTW: Toward accurate dynamic time warping in linear time and space.

Scipy.org, 2018, [Scipy.signal.correlate](https://docs.scipy.org/doc/scipy/reference/generated/scipy.signal.correlate.html), <https://docs.scipy.org/doc/scipy/reference/generated/scipy.signal.correlate.html>, accessed 16 July 2019.

Sollie, F. O. and S. G. Rodgers, 1994, Towards better measurements of logging depth, Paper SPWLA-1994-D presented at the SPWLA 35th Annual Logging Symposium, Tulsa, Oklahoma, USA, 19-22 June.

The HDF Group, 2016, High Level Introduction to HDF5, <https://support.hdfgroup.org/HDF5/Tutor/HDF5Intro.pdf>, accessed 1 September, 2019.

Theys, P. P., 1999, *Log data acquisition and quality control*, Editions Technip.

White, R. E., 1980, Partial coherence matching of synthetic seismograms with seismic traces, *Geophysical Prospecting*, **28**(03), 333-358. DOI: [10.1111/j.1365-2478.1980.tb01230.x](https://doi.org/10.1111/j.1365-2478.1980.tb01230.x).

White, R. and R. Simm, 2003, Tutorial: Good practice in well ties, *First Break*, **21**(10), 75-83. DOI: [10.3997/1365-2397.21.10.25640](https://doi.org/10.3997/1365-2397.21.10.25640).

Wilson, H., J. Lofts, G. Page, A. Brooks, and D. Walder, 2004, Depth control: Reconciliation of LWD and wireline depths, standard practice and an alternative simple but effective method, Paper SPE-89899-MS presented at the SPE Annual Technical Conference and Exhibition, Houston, Texas, USA, 26-29 September. DOI: [10.2118/89899-MS](https://doi.org/10.2118/89899-MS).

Zangwill, J., 1982, Depth Matching - A Computerized Approach, Paper SPWLA-1982-EE presented at SPWLA 23rd Annual Logging Symposium, Corpus Christi, Texas, USA, 6-9 July.

Zimmermann, T., Liang, L. & Zeroug, S., 2018, Machine-learning-based automatic well-log depth matching. *Petrophysics*, **59**(6), 863-872. DOI:10.30632/PJV59N6-2018a10.